γZ corrections to forward-angle parity-violating ep scattering

A. Sibirtsev,[1,2] P. G. Blunden,[3,2] W. Melnitchouk,[2] and A. W. Thomas[4]

[1]*Helmholtz-Institut für Strahlen- und Kernphysik (Theorie), Universität Bonn, D-53115 Bonn, Germany*
[2]*Jefferson Lab, 12000 Jefferson Avenue, Newport News, Virginia 23606, USA*
[3]*Department of Physics and Astronomy, University of Manitoba, Winnipeg, Manitoba, Canada R3T 2N2*
[4]*CSSM, School of Chemistry and Physics, University of Adelaide, Adelaide SA 5005, Australia*

(Received 3 February 2010; revised manuscript received 18 March 2010; published 30 July 2010)

We use dispersion relations to evaluate the γZ box contribution to parity-violating electron scattering in the forward limit arising from the axial-vector coupling at the electron vertex. The calculation makes full use of the critical constraints from recent JLab data on electroproduction in the resonance region as well as high-energy data from HERA. At the kinematics of the $Q_{\rm weak}$ experiment, this gives a correction of $0.0047^{+0.0011}_{-0.0004}$ to the standard model value 0.0713(8) of the proton weak charge. While the magnitude of the correction is highly significant, the uncertainty is within the anticipated experimental uncertainty of ± 0.003.

DOI: 10.1103/PhysRevD.82.013011 PACS numbers: 12.15.Lk, 13.60.Fz, 13.60.Hb, 14.20.Dh

Among the many methods for searching for physics beyond the standard model, the verification of the predicted evolution of the Weinberg angle from the Z pole to very low energies is currently of great interest. In particular, the $Q_{\rm weak}$ experiment at Jefferson Lab [1] is designed to measure the weak charge of the proton using parity-violating elastic electron scattering (PVES) from the proton to a higher level of precision than previously possible. In combination with constraints from atomic parity violation [2], $Q_{\rm weak}$ aims to either discover evidence for new physics beyond the standard model that leads to parity violation in electron scattering or raise the limit on its mass scale to above 2 TeV, complementing direct searches at the LHC [3,4].

In PVES the parity-violating asymmetry in the $t \to 0$ and low-energy limit is related to the weak charge of the proton Q_W^p [5]:

$$A^{\rm PV} \equiv \frac{\sigma_R - \sigma_L}{\sigma_R + \sigma_L} \to \frac{G_F}{4\pi\alpha\sqrt{2}} t Q_W^p, \tag{1}$$

where $\sigma_{L(R)}$ is the cross section for left-(right-)hand-polarized electrons, G_F is the Fermi constant, and α is the fine structure constant. The arrow serves to remind that this relation is only realized when radiative corrections are properly accounted for, in particular, any residual dependence on the electron energy E or the momentum transfer squared t. Including electroweak radiative corrections, the proton weak charge is defined at zero energy and momentum transfer as [4]

$$Q_W^p = (1 + \Delta\rho + \Delta_e)(1 - 4\sin^2\theta_W(0) + \Delta_e') + \Box_{WW} + \Box_{ZZ} + \Box_{\gamma Z}(0), \tag{2}$$

where $\sin^2\theta_W(0) = 0.238\,67(16)$ is the weak mixing angle at zero momentum, and the corrections $\Delta\rho$, Δ_e, and Δ_e' are given in [4] and references therein. The contributions $\Box_{WW}$ and $\Box_{ZZ}$ from the WW and ZZ box diagrams, respectively, can be computed perturbatively, while the γZ interference correction $\Box_{\gamma Z}(E)$ in addition depends on physics at low momentum scales [4–6]. The current best theoretical estimate from Ref. [4] is $Q_W^p = 0.0713(8)$.

In Eq. (2) we have explicitly introduced a dependence of $\Box_{\gamma Z}(E)$ on the electron energy E. The energy dependence of the other radiative corrections in Eq. (2) is not expected to be important at the $\mathcal{O}$(GeV) energies relevant for PVES. The Q_W^p extracted from $A^{\rm PV}$ in Eq. (1) will then differ from Q_W^p in Eq. (2) by an amount $\Box_{\gamma Z}(E) - \Box_{\gamma Z}(0)$, which we refer to in what follows as a correction to Q_W^p at the particular kinematics of the electron scattering experiment. In general, the γZ term has contributions from the vector electron–axial vector hadron coupling of the Z boson ($\Box_{\gamma Z}^A$) and from the axial vector electron–vector hadron coupling of the Z ($\Box_{\gamma Z}^V$), $\Box_{\gamma Z}(E) = \Box_{\gamma Z}^A(E) + \Box_{\gamma Z}^V(E)$.

Given that the $Q_{\rm weak}$ experiment has a precision target of 4.2% on Q_W^p [1], if we are to draw meaningful conclusions in relation to the standard model it is crucial that all the radiative corrections to PVES be under control at a level well below this target. The first studies of the box corrections [4–6] suggested that they were indeed understood to the required precision, with the uncertainty on the least constrained, $\Box_{\gamma Z}(0)$ term being 0.65%.

In their seminal early work, Marciano and Sirlin [6] computed the $\Box_{\gamma Z}^A(0)$ correction, which is dominant in atomic parity-violation experiments at very low electron energies. This correction was further divided into a high momentum contribution to the loop integral, computed at the quark level, and a low momentum contribution, computed with the nucleon elastic intermediate state. The entire uncertainty on the calculation was taken to arise from the low-energy component [4].

In a stimulating new analysis, Gorchtein and Horowitz [7] used forward-angle dispersion relations to evaluate the additional correction $\Box_{\gamma Z}^V(E)$, which is negligible at the low electron energies characteristic of atomic parity violation. However, at the $\mathcal{O}$(GeV) energies relevant for PVES

[1], this correction was found to be large, with an uncertainty potentially capable of jeopardizing the interpretation of the $Q_{\rm weak}$ experiment. Recent model-dependent analyses of the low-energy γZ contribution, involving only nucleon and Δ intermediate states, find smaller but non-negligible effects [8–10].

In this work we revisit this new $\Box^V_{\gamma Z}(E)$ radiative correction with a detailed evaluation of the inelastic contributions, taking full advantage of the wealth of data available in the resonance region and from deep-inelastic scattering (DIS) at high energy. We find that with these new experimental constraints the total $\Box^V_{\gamma Z}(E)$ contribution is quite well under control, constituting a correction of $0.0047^{+0.0011}_{-0.0004}$, or $6.6^{+1.5}_{-0.6}\%$, to Q^p_W at the $Q_{\rm weak}$ kinematics.

The $Q_{\rm weak}$ experiment is designed to measure the PVES asymmetry from protons at $E = 1.165$ GeV electron energy and very low momentum transfer squared, $-t = 0.026\ {\rm GeV}^2$ [1]. The purely electromagnetic and weak contributions are independent of the electron polarization, so that the asymmetry directly measures the parity-violating interference between the photon and Z exchange amplitudes.

For the $e(k) + N(p)$ elastic scattering process in the forward-angle limit, the Born amplitudes

$$\mathcal{M}_\gamma = \frac{1}{t}(-e2k_\mu)(+e2p^\mu) = -\frac{4\pi\alpha}{t}4k\cdot p, \tag{3}$$

$$\begin{aligned}\mathcal{M}^{\rm PV}_Z &= \left(\frac{-2G_F}{\sqrt{2}}\right)(-g^e_A 2k_\mu)\left(\frac{1}{2}Q^p_W 2p^\mu\right)\\ &= \frac{G_F}{\sqrt{2}}g^e_A Q^p_W 4k\cdot p\end{aligned} \tag{4}$$

depend only on the electron and proton convection currents. The PV Z exchange amplitude $\mathcal{M}^{\rm PV}_Z$ incorporates the difference between right- and left-polarized electron currents, so that $A^{\rm PV} = 2\mathcal{M}^*_\gamma\mathcal{M}^{\rm PV}_Z/|\mathcal{M}_\gamma|^2$ in Eq. (1) with $g^e_A = -1/2$ the weak axial charge of the electron.

The correction $\Box_{\gamma Z}$ in Eq. (2) arises from the replacement $\mathcal{M}^{\rm PV}_Z \to \mathcal{M}^{\rm PV}_Z + \mathcal{M}^{\rm PV}_{\gamma Z}$, so that

$$\Box_{\gamma Z} = Q^p_W\frac{\mathcal{M}^*_\gamma\mathcal{M}^{\rm PV}_{\gamma Z}}{\mathcal{M}^*_\gamma\mathcal{M}^{\rm PV}_Z}. \tag{5}$$

Corrections from the interference of $\mathcal{M}^{\rm PV}_Z$ with the two-photon exchange amplitude under the replacement $\mathcal{M}_\gamma \to \mathcal{M}_\gamma + \mathcal{M}_{\gamma\gamma}$ vanish in the $t \to 0$ limit and therefore do not affect the asymmetry.

Applying Cauchy's integral theorem, the real part of $\Box^V_{\gamma Z}(E)$ can be obtained from its imaginary part using a standard dispersion relation,

$${\rm Re}\,\Box^V_{\gamma Z}(E) = \frac{1}{\pi}P\int_{-\infty}^{\infty}dE'\frac{{\rm Im}\Box^V_{\gamma Z}(E')}{E'-E}, \tag{6}$$

where P is the principal value. The integration over negative energies corresponds to the crossed γZ box diagram, with the vector hadron correction even under $E' \to -E'$. Consequently ${\rm Re}\Box^V_{\gamma Z}(0) = 0$, justifying the neglect of this term at atomic scale electron energies. Following Ref. [7] we compute only the inelastic contributions to the dispersion integral; the elastic component has previously been computed to be small [6,8–10].

From the optical theorem, the imaginary part of PV γZ exchange amplitude $\mathcal{M}^{\rm PV}_{\gamma Z}$ can be written in terms of the cross section for all possible final hadronic states

$$\begin{aligned}2\,{\rm Im}\mathcal{M}^{\rm PV}_{\gamma Z} = 4\pi M\int\frac{d^3k'}{(2\pi)^3 2E_{k'}}\left(\frac{4\pi\alpha}{Q^2}\right)\left(\frac{-2G_F}{\sqrt{2}}\right)\\ \times\frac{1}{1+Q^2/M^2_Z}L^{\gamma Z}_{\mu\nu}W^{\mu\nu}_{\gamma Z},\end{aligned} \tag{7}$$

where $q = k - k'$ is the virtual four-momentum transfer (with $Q^2 = -q^2$), M (M_Z) is the proton (Z-boson) mass, and (neglecting the mass of the electron) $L^{\gamma Z}_{\mu\nu} = \frac{1}{2}{\rm Tr}[\gamma_\mu k'\gamma_\nu(g^e_V - g^e_A\gamma_5)\gamma_5 k]$ is the PV leptonic tensor arising from the difference between right- and left-polarized electrons. The symmetric part of the hadronic tensor

$$W^{\mu\nu}_{\gamma Z} = \frac{1}{4\pi M}\int d^4x e^{iq\cdot x}\langle p|[J^\mu_\gamma(x)J^\nu_Z(0) + J^\mu_Z(x)J^\nu_\gamma(0)]|p\rangle \tag{8}$$

can be written in terms of the interference electroweak $F^{\gamma Z}_{1,2}$ structure functions:

$$W^{\mu\nu}_{\gamma Z} = \frac{1}{M}\left[-F^{\gamma Z}_1 g^{\mu\nu} + F^{\gamma Z}_2\frac{p^\mu p^\nu}{p\cdot q}\right]. \tag{9}$$

Making a change of variables

$$\frac{d^3k'}{(2\pi)^3 2E_{k'}} \to \frac{1}{32\pi^2 k\cdot p}dW^2dQ^2, \tag{10}$$

and evaluating $k\cdot p = ME$ in the rest frame of the proton, we find for the g^e_A-dependent part:

$$\begin{aligned}{\rm Im}\,\Box^V_{\gamma Z}(E) = \frac{\alpha}{(s-M^2)^2}\int_{W^2_\pi}^{s}dW^2\int_0^{Q^2_{\rm max}}\frac{dQ^2}{1+Q^2/M^2_Z}\\ \times\left[F^{\gamma Z}_1 + F^{\gamma Z}_2\frac{s(Q^2_{\rm max}-Q^2)}{Q^2(W^2-M^2+Q^2)}\right],\end{aligned} \tag{11}$$

where $s = M(M + 2E)$ is the total c.m. energy squared. The structure functions $F^{\gamma Z}_{1,2}$ are functions of the exchanged boson virtuality Q^2 and of the invariant mass W of the exchanged boson and proton [or alternatively of the Bjorken variable $x = Q^2/(W^2 - M^2 + Q^2)$]. The lower

limit of the W integration is given by the mass $W_\pi = M + m_\pi$ of the pion production threshold, and the upper limit of the Q^2 integration is given by $Q^2_{\rm max} = 2ME(1 - W^2/s)$. Our definitions of the structure functions coincide with the standard definitions given by the Particle Data Group [11], in which at large Q^2 and W the $F_2^{\gamma Z}$ structure function, for example, can be written (at leading order) in terms of parton distributions q and $\bar{q}$ as

$$F_2^{\gamma Z} = x\sum_q 2e_q g_V^q (q + \bar{q}), \tag{12}$$

with weak vector charges $g_V^u = 1/2 - (4/3)\sin^2\theta_W$ and $g_V^d = -1/2 + (2/3)\sin^2\theta_W$ for u and d quarks, respectively. In particular, in the limit $2g_V^q \to e_q$ the interference structure functions $F_2^{\gamma Z} \to F_2^\gamma$ [11], where

$$F_2^\gamma = x\sum_q e_q^2 (q + \bar{q}). \tag{13}$$

We note that the expression (11) is a factor of 2 larger than that quoted in Ref. [7]. Because of the importance of this difference we have carried out a number of checks of our result. Most importantly, we have verified that Eq. (11) reproduces the known asymptotic limit for a pointlike hadron [6], as well as the independently calculated result for an elastic nucleon intermediate state [8–10]. We also point out that the relation between the structure functions and the virtual photon total cross sections used in [7] omits a factor $(1 - x)$ relative to the usual definition, which leads to an overestimate of the contribution by 30%–40% (and even more in the resonance region).

In the region of low intermediate state hadronic masses, $W \lesssim 2.5$ GeV, inclusive scattering is dominated by nucleon resonances. While there is an abundance of electroproduction data in the resonance region, there are no direct measurements of $F_{1,2}^{\gamma Z}$. For transitions to isospin $I = 3/2$ states, such as the Δ resonance, conservation of the vector current and isospin symmetry dictate that the weak isovector transition form factors are equal to the electromagnetic ones multiplied by $(1 + Q_W^p)$. For isospin $I = 1/2$ resonances, which contain contributions from isovector and isoscalar currents, using SU(6) quark model wave functions one can verify that for the most prominent $I = 1/2$ states the magnitudes of the Z-boson transition couplings are equal to the respective photon couplings to within a few percent.

Following the analyses of Refs. [12–14] we fit all of the available data, including the latest from Stanford Linear Accelerator Center (SLAC) [15] and JLab [16,17], using the isobar model for each Q^2, taking into account the contributions from four resonances: $P_{33}(1232)$, $D_{13}(1520)$, $F_{15}(1680)$, and $F_{37}(1950)$. The background contribution is taken to have the functional form $(1 - x)^\beta/x$, which allows

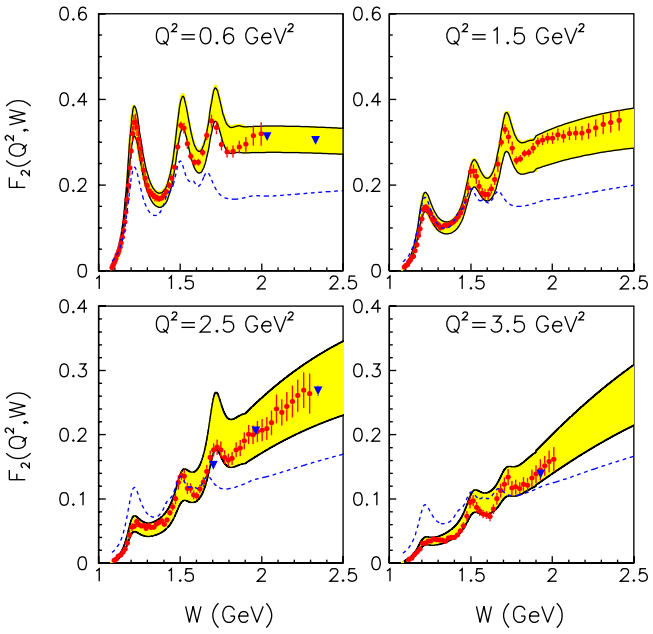

FIG. 1 (color online). Proton F_2 structure function versus W in the resonance region for fixed Q^2. The data are from JLab (circles) [16] and SLAC (triangles) [15]. The shaded (yellow) band between the solid lines represents the uncertainty on our fit, while the dashed lines are obtained by summing the resonance fit from Ref. [19] and the nonresonant contributions from Ref. [20].

for a smooth transition to the large-W region. The fit allows the inclusive transition form factors for each of the resonances to be constrained accurately up to $Q^2 \approx 3$ GeV^2. At larger Q^2, where the resonance transitions are not as well determined, we extrapolate the form factors using an exponential form [18]. This introduces a relatively small uncertainty, as the resonance contributions are strongly suppressed at large Q^2.

The results of our fit for the F_2 structure function are shown in Fig. 1 as a function of W for several values of Q^2, together with the uncertainties associated with the parameters of the fit. For comparison, we also show the results obtained by adding the contributions from resonances parametrized in Ref. [19] and the background from Ref. [20], which were used in the analysis of Ref. [7]. The resonance parametrization [19] fixes the fit parameters from data at the real photon point, $Q^2 = 0$. To obtain transverse and longitudinal cross sections, the Q^2 dependence was inferred in Ref. [7] using a simple ansatz. Comparison with the data in Fig. 1 shows that this parametrization does not adequately reproduce the experimental results in the resonance region.

In the DIS region the interference structure functions can be expressed in terms of leading twist parton distribution functions (PDFs). However, the range of integration in Eq. (11) extends to low W and Q^2, beyond the region of validity of a PDF description. To proceed we follow Ref. [7] and approximate $F_{1,2}^{\gamma Z}$ by their electromagnetic

analogs $F_{1,2}$ at very small x where the light-quark PDFs are approximately flavor-independent. Here the structure functions are proportional to a sum over products of weak and electric charges, which for three flavors are approximately equal [7,11].

For F_2 we use the parametrization from Refs. [21,22], which is motivated by Regge theory and valid at both high Q^2 and low Q^2,

$$F_2(x, Q^2) = A_P x^{-\Delta}(1-x)^{n+4}\left[\frac{Q^2}{Q^2+\Lambda_P^2}\right]^{1+\Delta} + A_R x^{1-\alpha_R}(1-x)^{n}\left[\frac{Q^2}{Q^2+\Lambda_R^2}\right]^{\alpha_R}, \quad (14)$$

where the first term accounts for the Pomeron contribution, while the second arises from an effective Reggeon exchange. The parameters, and the Q^2 dependence of the exponents n and Δ, are given in Ref. [21], with a couple of minor adjustments to better fit the high-Q^2 HERA data [23] and the Martin-Roberts-Stirling-Thorne (MRST) leading twist fit [24] (viz., the normalization of Δ increased by 8% and its Q^2 cutoff mass decreased by 5% relative to [21]).

At larger x ($x \gtrsim 0.4$) the flavor dependence of the PDFs renders the interference function ~30%–40% smaller than F_2. The electromagnetic structure functions therefore provide an upper limit on $F_2^{\gamma Z}$. However, to obtain a more accurate estimate, we use $F_2^{\gamma Z} = (F_2^{\gamma Z}/F_2)^{\rm LT} F_2$, with F_2 given by Eq. (14) and the leading twist (LT) ratio constructed from the MRST PDFs [24]. As Figs. 2 and 3 demonstrate, this procedure yields a very good description of the W dependence of the available SLAC, NMC, and H1 data [15,25,26] in the kinematics most relevant for $\Box^V_{\gamma Z}(E)$ and also gives an excellent description of the ZEUS data up to $Q^2 \approx 90$ GeV^2 [27]. The fit (14) in the DIS region also agrees well with the MRST parameterization [24] of F_2. In contrast, the generalized vector dominance color dipole model [20], used in the calculation of Ref. [7], slightly underestimates the data at lower W but exceeds the other fits above $W \sim 100$ GeV.

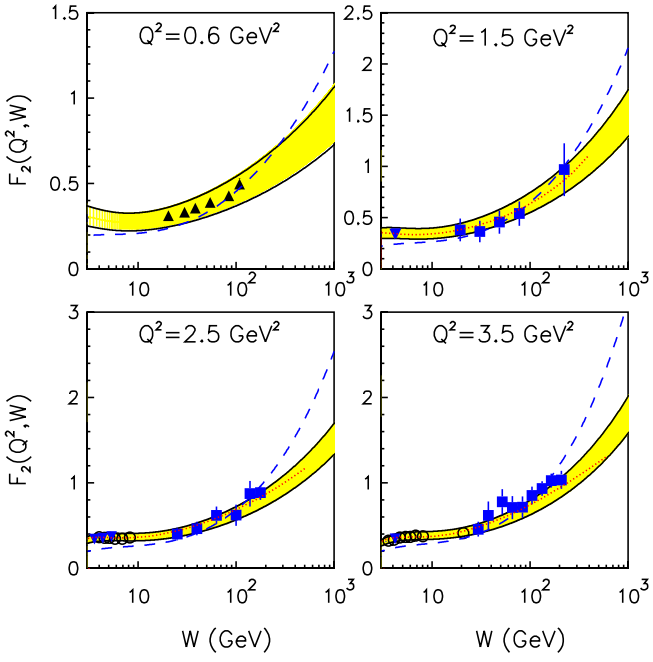

FIG. 2 (color online). As in Fig. 1 but for higher values of W. The data are from SLAC (triangles) [15], NMC (circles) [25], and H1 (squares) [26]. The solid lines show the fit [21,22] used in this analysis, with the (yellow) bands representing the uncertainty. The dashed lines are the results of the generalized vector dominance color dipole model [20], while the dotted lines represent the MRST leading twist fit [24].

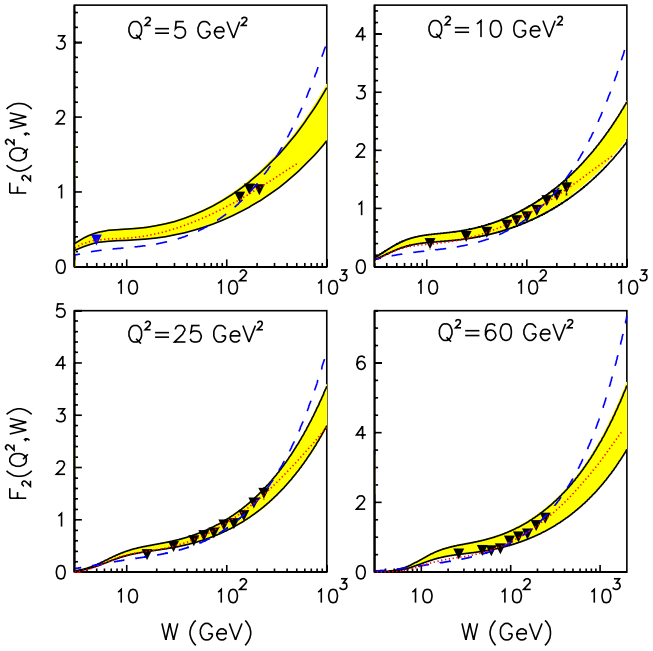

FIG. 3 (color online). As in Fig. 2 but for $Q^2 = 5$, 10, 25, and 60 GeV^2.

The contribution from the F_1 structure function to $\mathrm{Im}\Box^V_{\gamma Z}(E)$ is obtained from F_2 and the ratio $R = \sigma_L/\sigma_T = (1 + 4M^2x^2/Q^2)F_2/(2xF_1) - 1$ of the longitudinal and transverse cross sections. The latter has been measured only over a limited range of x and Q^2; however, its contribution is numerically small, especially at large Q^2 and W. We use the parameterization $R = c_1 Q^2(\exp(-c_2 Q^2) + c_3 \exp(-c_4 Q^2))$, with $c_{1-4} = \{0.014, 0.07, 41, 0.8\}$, which provides a good description of available data and has the correct photoproduction and high-energy limits. This parametrization compares favorably with the earlier SLAC fit [28], which included a mild x dependence, but was restricted to $Q^2 \gtrsim 0.3$ GeV^2.

Performing the dispersion integration in Eq. (6), the result for $\mathrm{Re}\Box^V_{\gamma Z}(E)$ is shown in Fig. 4 as a function of the incident electron energy E. Although the integration in principle involves an infinite range of W and Q^2, in practice we find that around 80% of the value of $\mathrm{Re}\Box^V_{\gamma Z}(E)$ at

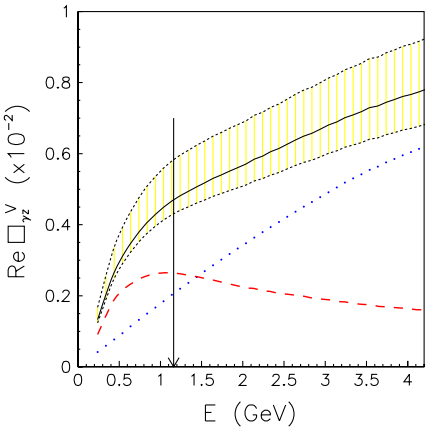

FIG. 4 (color online). γZ box correction $\Box^V_{\gamma Z}(E)$ to Q^p_W as a function of electron energy E, showing the resonant (dashed line) and nonresonant (dotted line) contributions, as well as the sum (solid line) and the overall (asymmetric) uncertainty (shaded area). The vertical arrow at $E = 1.165$ GeV indicates the energy of the $Q_{\rm weak}$ experiment.

the energy relevant to $Q_{\rm weak}$ comes from energies below 4 GeV, where the Q^2 range extends to $\sim$6 GeV^2 and W to $\sim$3 GeV. This is fortunate as it is precisely in this region that a wealth of very accurate data exists from JLab [16,17].

In Fig. 4 the nonresonant contribution is small at low energies but rises logarithmically with increasing E. The resonance contribution increases steeply to a maximum at $E \sim 1$ GeV, before falling off like $1/E$. The resonant and nonresonant contributions to $\mathrm{Re}\Box^V_{\gamma Z}(E)$ are 0.0026 and 0.0021, respectively, at the energy relevant for the $Q_{\rm weak}$ experiment, $E = 1.165$ GeV. We should note, however, that this separation is somewhat arbitrary, as only the physically meaningful, total cross section enters into our fit.

The combined correction to Q^p_W at the $Q_{\rm weak}$ energy is then $0.0047^{+0.0011}_{-0.0004}$, or $6.6^{+1.5}_{-0.6}\%$ of the standard model value 0.0713(8) for Q^p_W, with the error band obtained from the uncertainty in the fit parameters using a variational method. In comparison, the correction found in Ref. [7] was ≈ 0.003. The major difference with our value arises from the additional factor 2 in Eq. (11), which has been verified by the independent checks discussed earlier, as well as our use of more recent electroproduction data and the correct relation between structure functions and the virtual photon cross section. The correction is important for the interpretation of the $Q_{\rm weak}$ experiment, given its projected uncertainty of ± 0.003 [1]. It is also critical to the physical interpretation of the experiment which is expected to constrain possible sources of parity violation from beyond the standard model at a mass scale of $\gtrsim 2$ TeV [3]. While the uncertainty in the result reported here is satisfactory from the point of view of $Q_{\rm weak}$, it can be further reduced by incorporating the new inclusive parity-violating data in the resonance region which should be taken soon at JLab [29].

We thank R. Carlini, M. Gorchtein, D. Schildknecht, and W. van Oers for helpful discussions and communications. This work was supported by DOE Contract No. DE-AC05-06OR23177, under which Jefferson Science Associates, LLC operates Jefferson Lab, NSERC (Canada), and the Australian Research Council through an Australian Laureate Fellowship (A. W. T.).

[1] JLab experiment E-08-016 ($Q_{\rm weak}$), R. D. Carlini *et al.*, spokespersons.
[2] S. G. Porsev, K. Beloy, and A. Derevianko, Phys. Rev. Lett. **102**, 181601 (2009).
[3] R. D. Young, R. D. Carlini, A. W. Thomas, and J. Roche, Phys. Rev. Lett. **99**, 122003 (2007).
[4] J. Erler, A. Kurylov, and M. J. Ramsey-Musolf, Phys. Rev. D **68**, 016006 (2003); J. Erler and M. J. Ramsey-Musolf, Phys. Rev. D **72**, 073003 (2005).
[5] M. J. Musolf *et al.*, Phys. Rep. **239**, 1 (1994).
[6] W. J. Marciano and A. Sirlin, Phys. Rev. D **27**, 552 (1983); **29**, 75 (1984); **31**, 213(E) (1985).
[7] M. Gorchtein and C. J. Horowitz, Phys. Rev. Lett. **102**, 091806 (2009).
[8] H. Q. Zhou, C. W. Kao, and S. N. Yang, Phys. Rev. Lett. **99**, 262001 (2007).
[9] J. A. Tjon and W. Melnitchouk, Phys. Rev. Lett. **100**, 082003 (2008).
[10] J. A. Tjon, P. G. Blunden, and W. Melnitchouk, Phys. Rev. C **79**, 055201 (2009).
[11] C. Amsler *et al.*, Phys. Lett. B **667**, 1 (2008).
[12] A. A. Cone *et al.*, Phys. Rev. **156**, 1490 (1967).
[13] S. Stein *et al.*, Phys. Rev. D **12**, 1884 (1975).
[14] F. W. Brasse *et al.*, Nucl. Phys. **B110**, 413 (1976).
[15] L. W. Whitlow *et al.*, Phys. Lett. B **282**, 475 (1992).
[16] M. Osipenko *et al.*, Phys. Rev. D **67**, 092001 (2003).
[17] I. Niculescu *et al.*, Phys. Rev. Lett. **85**, 1186 (2000); Y. Liang *et al.*, arXiv:nucl-ex/0410027; S. P. Malace *et al.*, Phys. Rev. C **80**, 035207 (2009).
[18] V. M. Braun, A. Lenz, G. Peters, and A. V. Radyushkin, Phys. Rev. D **73**, 034020 (2006).
[19] N. Bianchi *et al.*, Phys. Rev. C **54**, 1688 (1996).
[20] G. Cvetic, D. Schildknecht, B. Surrow, and M. Tentyukov, Eur. Phys. J. C **20**, 77 (2001).
[21] A. Capella, A. Kaidalov, C. Merino, and J. Tran Thanh Van, Phys. Lett. B **337**, 358 (1994).

[22] A. B. Kaidalov and C. Merino, Eur. Phys. J. C **10**, 153 (1999).
[23] M. Derrick *et al.*, Z. Phys. C **72**, 399 (1996).
[24] A. D. Martin, R. G. Roberts, W. J. Stirling, and R. S. Thorne, Eur. Phys. J. C **28**, 455 (2003).
[25] P. Amaudruz *et al.*, Phys. Lett. B **295**, 159 (1992).
[26] S. Aid *et al.*, Nucl. Phys. **B468**, 3 (1996).
[27] J. Breitweg *et al.*, Phys. Lett. B **487**, 53 (2000).
[28] L. W. Whitlow *et al.*, Phys. Lett. B **250**, 193 (1990).
[29] JLab experiments E-05-007, R. Michaels, P. Reimer, and X. Zheng, spokespersons and E12-07-102, K. Paschke, P. Reimer, and X. Zheng, spokespersons.